Structure of a patient-derived antibody in complex with allergen reveals simultaneous conventional and superantigen-like recognition

Alkistis N. Mitropoulou[a,1], Holly Bowen[a,b,c], Tihomir S. Dodev[a,b], Anna M. Davies[a,b], Heather J. Bax[a,b], Rebecca L. Beavil[a,b], Andrew J. Beavil[a,b], Hannah J. Gould[a,b], Louisa K. James[a,b,d,2], and Brian J. Sutton[a,b,2]

[a]Randall Centre for Cell and Molecular Biophysics, King's College London, SE1 1UL London, United Kingdom; [b]Medical Research Council and Asthma UK Centre in Allergic Mechanisms of Asthma, SE1 1UL London, United Kingdom; [c]National Institute for Health Research Biomedical Research Centre at Guy's and St. Thomas' National Health Service Foundation Trust, King's College London, SE1 1UL London, United Kingdom; and [d]Blizard Institute, Barts and the London School of Medicine, Queen Mary University of London, E1 2AT London, United Kingdom

Antibodies classically bind antigens via their complementarity-determining regions, but an alternative mode of interaction involving V-domain framework regions has been observed for some B cell "superantigens." We report the crystal structure of an antibody employing both modes of interaction simultaneously and binding two antigen molecules. This human antibody from an allergic individual binds to the grass pollen allergen *Phl p* 7. Not only are two allergen molecules bound to each antibody fragment (Fab) but also each allergen molecule is bound by two Fabs: One epitope is recognized classically, the other in a superantigen-like manner. A single allergen molecule thus cross-links two identical Fabs, contrary to the one-antibody–one-epitope dogma, which dictates that a dimeric allergen at least is required for this to occur. Allergens trigger immediate hypersensitivity reactions by cross-linking receptor-bound IgE molecules on effector cells. We found that monomeric *Phl p* 7 induced degranulation of basophils sensitized solely with this monoclonal antibody expressed as an IgE, demonstrating that the dual specificity has functional consequences. The monomeric state of *Phl p* 7 and two structurally related allergens was confirmed by size-exclusion chromatography and multiangle laser light scattering, and the results were supported by degranulation studies with the related allergens, a second patient-derived allergen-specific antibody lacking the nonclassical binding site, and mutagenesis of the nonclassically recognized allergen epitope. The antibody dual reactivity and cross-linking mechanism not only have implications for understanding allergenicity and allergen potency but, importantly, also have broader relevance to antigen recognition by membrane Ig and cross-linking of the B cell receptor.

antibody structure | allergen | IgE | basophil degranulation | superantigen-like recognition

The recognition of antigens by antibodies classically involves the complementarity-determining regions (CDRs) of the antibody heavy-chain variable (VH) and light-chain variable (VL) domains. However, alternative modes of antibody–antigen interaction involving residues of the V domain framework regions (FRs) have been reported: *Staphylococcal* Protein A and *Peptostreptococcal* Protein L, for example, bind to FRs of VH and VL domains, respectively (1, 2). These molecules are termed "B cell superantigens" because, in polymeric form, they can cross-link the surface Ig molecules of the B cell receptor (BCR) independently of CDR-mediated antigen binding. This is analogous to the bacterial enterotoxins known as "T cell superantigens" that bind to both T cell receptor (TCR) V domains and MHC molecules, bypassing CDR-mediated TCR recognition of MHC-bound antigen and activating T cells in a nonspecific manner (3). We have discovered an antibody that not only employs both "classical" (CDR-mediated) and superantigen-like (FR-mediated) recognition of the same protein antigen but also can bind two molecules of the antigen simultaneously.

The antibody is derived from an allergic individual (4) and recognizes the Timothy grass-pollen allergen *Phl p* 7. Allergic sensitization occurs when allergen-specific IgE molecules bind to effector cells such as mast cells and basophils via the high-affinity receptor FcεRI. Cross-linking of receptor-bound IgE by allergen leads to cell activation, degranulation, and release of preformed mediators of inflammation, causing an immediate hypersensitivity reaction and the characteristic manifestations of a range of allergic conditions including allergic asthma, rhinitis (hay fever), and food allergies (5). *Phl p* 7 is a highly cross-reactive "pan-allergen" (6) whose structure has been determined in solution by NMR and X-ray crystallography (7, 8). It is a member of the polcalcin family and consists of two calcium-binding EF-hand motifs in each molecule; the EF-hand is a 30-residue motif with a characteristic structure consisting of a central metal ion-binding

Significance

We have discovered that a human antibody can simultaneously bind two molecules of antigen, in this case a grass pollen allergen, one in a conventional manner and the other unconventionally. The two allergen molecules also bridge two identical antibodies. These observations challenge the dogma that one antibody recognizes only a single antigen/allergen epitope. The mechanism of antibody cross-linking seen here may explain the potency of certain allergens in triggering an allergic reaction, extending our understanding of the nature of allergenicity and informing the design of hypoallergenic molecules for allergen immunotherapy. This dual reactivity and potential for cross-linking surface immunoglobulin on B cells suggests mechanisms by which human autoimmune and other diseases might be initiated.

IMMUNOLOGY AND INFLAMMATION

loop flanked by two helices (E and F). The NMR structure of *Phl p* 7 is monomeric (7); however, the crystal structure revealed a domain-swapped dimer (8). In the absence of calcium, conformational changes occur (7, 8) which can affect recognition by IgE (9); in the case of the antibody studied here, the subnanomolar binding affinity for calcium-bound *Phl p* 7 is reduced 10,000-fold in the absence of calcium (4).

In the crystal structure reported here, each antibody fragment (Fab) molecule binds two monomeric *Phl p* 7 molecules, and each *Phl p* 7 monomer bridges two Fabs. Despite its small size, the two epitopes on *Phl p* 7, one recognized classically and the other in a superantigen-like manner, do not overlap; a single molecule of monomeric allergen could thus cross-link two identical antibodies, as seen in the crystal structure. This is counter to the current dogma of "one-antibody–one-epitope," which implies that cross-linking of identical antibodies is possible only if the antigen (allergen) presents more than one copy of the epitope, that is, it must be at least a dimer or have duplicated domains. The common occurrence of dimeric allergens has been highlighted (10–12), and two crystal structures have shown allergen dimers cross-linking two identical Fabs (13, 14). If, however, the cross-linked IgE molecules are of different specificity and recognize different epitopes, then, depending on the relative disposition of the epitopes, a monomeric allergen could cause cross-linking. This has been investigated recently, and cross-linking has been demonstrated in a model system (15).

We show here in a basophil degranulation assay that monomeric *Phl p* 7 allergen can indeed cross-link identical patient-derived monoclonal antibodies expressed as IgE, as seen in the crystal structure, by virtue of this combination of both conventional and superantigen-like recognition. Our unexpected result may account for the potency of this and other allergens, broadens our understanding of the molecular basis of allergenicity and antigenicity in general, and has implications for designing hypoallergenic molecules for allergen immunotherapy. Furthermore, the dual reactivity and superantigen-like activity also suggests a previously unanticipated mechanism for cross-linking surface Ig molecules in the BCR, which may explain aberrant B cell activation in autoimmune and other conditions.

Results

Phl p 7-Specific Antibodies and Their Cross-Reactivity for Related Polcalcins.
Two *Phl p* 7-specific antibodies, 102.1F10 and CS09G6K, were generated from matched heavy- and light-chain sequences by single B cell cloning from allergic individuals (*Materials and Methods*) (4). Both antibodies, initially derived as IgG4 and IgG2, respectively, were expressed as IgE antibodies to study the cross-linking of receptor-bound IgE molecules by *Phl p* 7 and other polcalcin allergens. 102.1F10 was additionally expressed as an IgG1 Fab for structural and binding studies.

There is substantial antibody cross-reactivity among the polcalcins (16). The affinities of 102.1F10 IgE and CS09G6K IgE for three polcalcins, *Phl p* 7, *Ole e* 3, and *Bet v* 4, were determined by surface plasmon resonance (SPR) analysis (*SI Appendix*, Fig. S1 *A* and *B*); the affinity of 102.1F10 Fab for each of the three polcalcins was similarly measured and found to be virtually identical to those for the IgE (*SI Appendix*, Fig. S1*C*). The sequence similarity between *Phl p* 7 and *Ole e* 3 is 68%, and these two allergens showed similarly high affinities for both IgE antibodies (*SI Appendix*, Fig. S1*D*). *Bet v* 4, which also has 68% sequence similarity to *Phl p* 7, was bound 1,000-fold more weakly than *Phl p* 7 by 102.1F10 IgE and Fab, and there was no detectable binding with CS09G6K IgE (*SI Appendix*, Fig. S1). However, there are no structural data for complexes of any of these other polcalcin allergens with their specific antibodies to shed light on the precise details of the recognition of their epitopes.

Crystal Structure of the *Phl p* 7/Fab Complex.
We solved the structure of the complex between 102.1F10 Fab and *Phl p* 7 at 2.35-Å resolution; X-ray data processing and refinement statistics are presented in *SI Appendix*, Table S1. Two Fab molecules and two monomeric *Phl p* 7 molecules were found in the asymmetric unit, with each Fab binding to two *Phl p* 7 molecules (Fig. 1*A*). The two (essentially identical) *Phl p* 7 molecules, which do not contact one another, independently bridge the two (essentially identical) Fabs (Fig. 1*A*). Each allergen molecule links the two Fabs using two distinct interaction sites; these two different sites can be seen for one of the *Phl p* 7 molecules in an orthogonal view (Fig. 1*B*). The other *Phl p* 7 molecule similarly links the two Fabs using an identical pair of interaction sites. These two interaction sites involve distinct (nonoverlapping) epitopes on the allergen and distinct (nonoverlapping) binding sites on the antibody. Thus, each *Phl p* 7 molecule is bound simultaneously by two antibody Fabs, and each Fab simultaneously binds two *Phl p* 7 molecules. One of these sites on the antibody is the classic antigen-binding site involving the CDRs (Fig. 1 *C* and *D*), while the other, unexpected site, which we term "nonclassical", involves FR residues outside the CDRs (Fig. 1 *E* and *F*). These interaction sites are described in detail below.

Interpretable electron density was present for residues Gln1–Thr214 in the light chains and Gln1–Lys222 in the heavy chains of both 102.1F10 Fabs and Asp4–Met71 or –Lys72 in the two *Phl p* 7 molecules. Clear density was also observed for the two calcium ions in each *Phl p* 7 molecule. No electron density was observed for the first three residues of either *Phl p* 7 molecule, for the last six and seven C-terminal residues, or for the C-terminal tag (V5-His tag) in either *Phl p* 7 molecule, although mass spectrometry analysis on the protein from which crystals were grown showed that the tag had been cleaved only partially.

The classical binding site of 102.1F10 Fab involves all three CDRs of the heavy chain and CDR-L1 and CDR-L3 of the light chain. The Fab contacts the F-helix of the N-terminal EF-hand, the E-helix of the C-terminal EF-hand [consistent with earlier epitope mapping in solution (16)], and residues Lys19 and Asp48 and Asp50 and Phe54 of Ca^{2+}-binding loops 1 and 2, respectively (Fig. 1*C*). Interactions include hydrogen bonds, π–π contacts between aromatic rings, and π–cation interactions (Fig. 1*D*). The interface area is ~830 $Å^2$, with contacts made by the heavy chain of 102.1F10 Fab constituting over 70% of the interface area, as calculated using PISA (17). CDR-H3, which has an extended conformation toward the allergen surface, contributes most of these contacts as expected of a classical binding site.

The other, nonclassical binding site of 102.1F10 Fab involves the light chain alone, more specifically three CDR-L2 residues and three adjacent FR-L3 residues (Fig. 1*E*). The other CDRs do not contribute to this binding interaction at all. Seven hydrogen bonds, a salt bridge, and cation–π interactions are formed between the Fab and *Phl p* 7 at this site (Fig. 1*F*), which involves the N-terminal E-helix and Ca^{2+}-binding loop 1 of the allergen. The interface area is ~330 $Å^2$, more than 30% of which is contributed by three residues which involve a salt bridge between Arg7 of *Phl p* 7 and Asp62 and a hydrogen bond to Thr78, both FR-L3 residues. Asn55 in CDR-L2 also plays an important role in this nonclassical interaction, forming two hydrogen bonds with the allergen. Another two asparagine residues in CDR-L2, Asn53 and Asn54, form hydrogen bonds with residues Asn15 and Thr14 of the allergen, respectively.

The crystal structure thus reveals an antibody Fab binding two antigen (allergen) molecules simultaneously and a monomeric allergen bridging two Fabs of identical specificity (Fig. 1 *A* and *B*). Contrary to current thinking, this implies that a monomeric allergen can cross-link two identical receptor-bound IgE molecules. We therefore investigated the functional consequences of this interaction for basophil degranulation by monomeric *Phl p* 7.
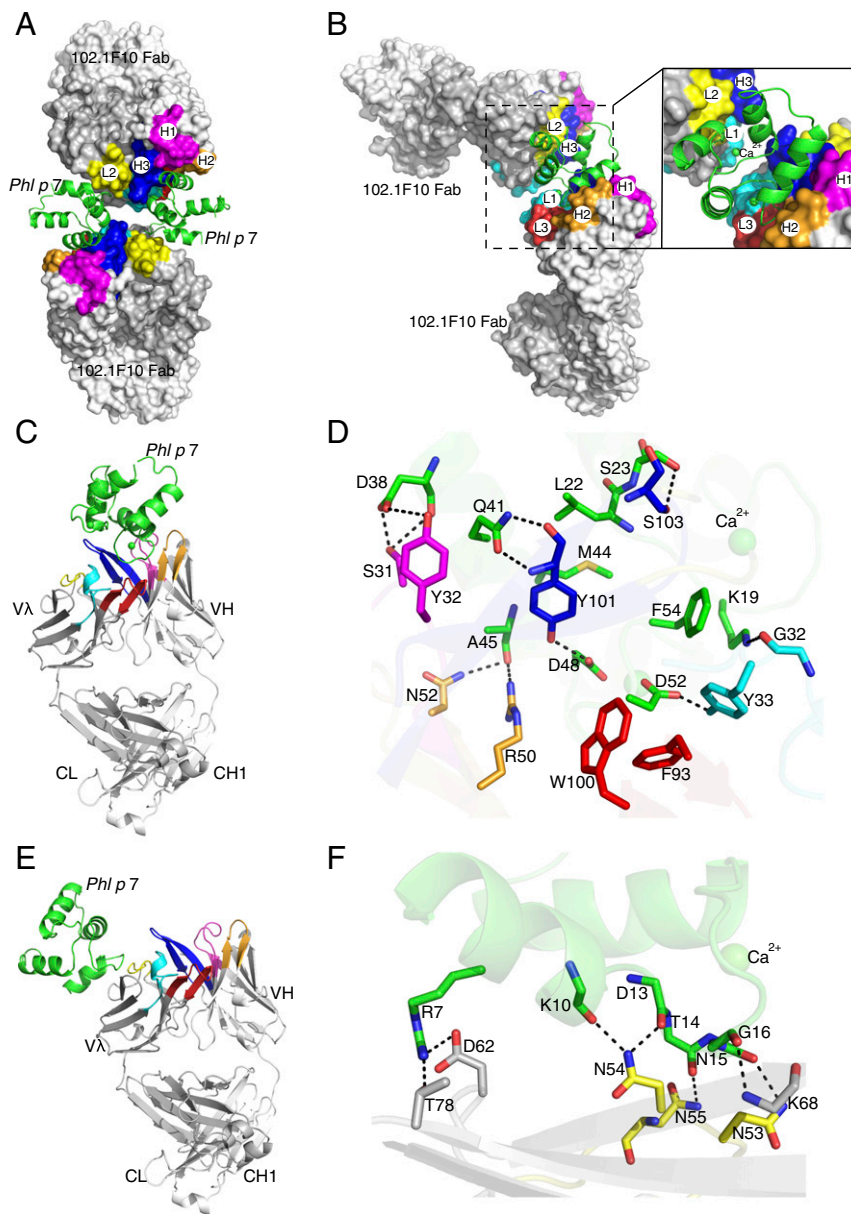
Fig. 1. The crystal structure of *Phl p* 7 in complex with 102.1F10 Fab reveals two monomeric allergen molecules bound independently to two identical Fabs. The Fabs are shown in white and light gray; CDRs H1, H2, and H3 are labeled and colored magenta, orange, and blue, respectively; CDRs L1, L2, and L3 are labeled and colored cyan, yellow, and red, respectively; *Phl p* 7 is shown in green; calcium ions are shown as green spheres. (*A*) The overall structure of the complex: *Phl p* 7 (green cartoon) and Fabs (white/gray surfaces) with colored CDRs. (*B*) Orthogonal orientation with respect to *A* showing one of the *Phl p* 7 molecules and details (enlarged view) of its different mode of binding to each of the two identical Fabs: nonclassical interaction above and classical interaction below. (*C*) The classical binding interaction between *Phl p* 7 and Fab showing involvement of the CDRs. (*D*) Details of the classical interaction showing hydrogen bonds (dashed lines) with residues colored according to the code described above. (*E*) The nonclassical binding interaction between *Phl p* 7 and Fab involving light chain FR and CDR-L2 residues. (*F*) Details of the nonclassical interaction showing hydrogen bonds (dashed lines) with residues colored according to the code described above. A salt bridge between Arg7 of *Phl p* 7 and Fab light-chain FR residue Asp62 is shown.

Basophil Degranulation by Monomeric Polcalcins. *Phl p* 7, together with *Ole e* 3 and *Bet v* 4, were tested for their ability as monomeric proteins to cause degranulation of basophils sensitized with either 102.1F10 IgE or CS09G6K IgE. Studies on other families of allergens, for example the profilins, have shown that many allergens naturally dimerize. However, biophysical studies of polcalcins *Phl p* 7 and *Bet v* 4, including NMR structure determinations, have reported that these allergenic molecules are monomeric in solution (7, 18, 19), although hydrodynamic studies of the latter showed a minor dimeric component. In contrast, crystallographic studies of *Phl p* 7 (8) and another

polcalcin *Che a* 3 revealed domain-swapped dimers, although these were formed under nonphysiological conditions of low pH; for the latter, mass spectrometry revealed a minor component of dimer in solution (20). *Phl p* 7 has also been shown to undergo temperature-dependent dimerization, but this is only reported to occur at nonphysiological temperatures (75 °C) (21). In the crystal structure reported here, *Phl p* 7 bound to 102.1F10 Fab remains monomeric, despite the relatively high protein concentration and long incubation time required for crystallization.

Size-exclusion chromatography with multiangle laser light scattering (SEC-MALLS) was used to determine the oligomeric

state of the three allergens in solution at physiological pH (Fig. 2A). *Phl p* 7 was injected at a concentration of 8 mg/mL. The mass of *Phl p* 7 (corresponding to the peak in the chromatograms, eluting at around 2 min) is 12.4 ± 1.1 kDa, in agreement with the calculated value of 12.5 kDa. *Bet v* 4 was injected at 0.8 mg/mL (at the lower detectable concentration range of the SEC-MALLS system; see *Materials and Methods*) and *Ole e* 3 at 3.6 mg/mL; the experimental values of 12.0 ± 1.4 kDa and 12.4 ± 1.0 kDa, respectively, agree with the calculated values of 13.4 kDa and 13.3 kDa. Complex formation between *Phl p* 7 and 102.1F10 IgE was also monitored by SEC-MALLS (*SI Appendix*, Fig. S2).

The allergens were purified immediately before the basophil degranulation assay, and the monomeric state of each was confirmed using SEC-MALLS (Fig. 2A). Additionally, a sample of each protein was incubated at 37 °C until the completion of the basophil degranulation assay for a second SEC-MALLS analysis; these measurements revealed that all three polcalcins remained monomeric during the time course of the degranulation assay; no aggregates or higher-order species were detected (*SI Appendix*, Fig. S3).

Basophil degranulation was assessed by β-hexosaminidase release, expressed as a percentage of that induced by cell lysis (*Materials and Methods*). RBL-SX38 cells, which express human

Fig. 2. Characterization of oligomeric state and basophil degranulation for the three polcalcin allergens. (*A*) Chromatograms of the RI signals for *Phl p* 7, *Bet v* 4, and *Ole e* 3. The three proteins [in 25 mM Tris·HCl (pH 7.4) and 150 mM NaCl with 4 mM CaCl₂] were run over a Superdex 75 5/150 column (GE Healthcare) at a flow rate of 0.3 mL/min. The differential RI is shown in black (A.U., arbitrary units). The green lines across the protein elution volumes show the molecular masses of the proteins, indicating a monomeric state. (*B*) Basophil degranulation assay showing the percentage degranulation of RBL-SX38 cells sensitized with 102.1F10 IgE (black bars) and CS09G6K IgE (white bars) antibodies followed by stimulation with 5,000 ng/μL of *Phl p* 7, *Bet v* 4, or *Ole e* 3 or with assay medium (background). Degranulation is expressed as a percentage of that induced by cell lysis. Bars represent the mean ± SEM of three independent experiments. Statistical significance was determined by *t* test; ****$P < 0.0001$.

FcεRI, were sensitized with 102.1F10 or CS09G6K *Phl p* 7-specific IgE and then were stimulated with 50, 500, or 5,000 ng/mL of allergen (the 5,000 ng/mL point is shown in Fig. 2*B*). Both *Phl p* 7 and *Ole e* 3, but not *Bet v* 4, induced degranulation of basophils sensitized with 102.1F10 IgE. While *Bet v* 4 has high sequence similarity to *Phl p* 7 and *Ole e* 3, and all three are presumably recognized classically by 102.1F10 IgE in a similar way (indeed, all the residues involved in the nonclassical site are conserved in all three polcalcins), *Bet v* 4 binding at the classical site is substantially weaker (*SI Appendix*, Fig. S1*A*), the likely cause of its failure to cause degranulation. None of the three polcalcins induced degranulation of basophils sensitized with CS09G6K IgE (Fig. 2*B*). (The ability of *Phl p* 7 to induce basophil degranulation was tested with three *Phl p* 7 protein constructs: N-terminal–tagged, C-terminal–tagged, and N-terminal tag–cleaved. All three constructs, which are monomeric proteins, induced degranulation of basophils sensitized with 102.1F10 IgE but not with CS09G6K IgE. The tag therefore has no impact on the activity of the protein).

The inability of *Phl p* 7 to induce degranulation of basophils sensitized with CS09G6K IgE supports the involvement of the nonclassical interaction with 102.1F10 IgE in basophil degranulation induced by monomeric *Phl p* 7. Both antibodies bind *Phl p* 7 with high affinity (*SI Appendix*, Fig. S1) at overlapping epitopes as demonstrated by competition SPR experiments, but CS09G6K IgE expresses a Vκ rather than the Vλ light chain of 102.1F10 IgE. None of the six residues in CDR-L2 or FR-L3 of 102.1F10 IgE involved in the nonclassical interaction is present in CS09G6K IgE.

Mutation of the Nonclassical Binding Site Abrogates Basophil Degranulation. To test the proposed involvement of the nonclassical site in IgE cross-linking, a point mutation was made in *Phl p* 7, replacing Arg7, which forms a key salt bridge with Asp62 of FR-L3 of 102.1F10 Fab at the nonclassical binding site (Fig. 1*F*), with threonine. This mutation would disrupt the salt bridge and would be expected to severely compromise the nonclassical interaction but not affect the folding of the allergen or its ability to be recognized by 102.1F10 IgE through the classical binding interaction. Indeed, the *Phl p* 7 R7T mutant was shown to be folded and monomeric by 1D ^{1}H-NMR and SEC-MALLS (Fig. 3*A*), respectively. *Phl p* 7 R7T was also shown to bind 102.1F10 IgE by SPR analysis, presumably at the classical site, with a fourfold reduction in affinity ($K_d = 6 \times 10^{-10}$ M) compared with the wild-type protein (Fig. 3*B*); this reduced affinity is a consequence of a slightly faster dissociation rate. *Phl p* 7 R7T did not induce degranulation of RBL-SX38 cells sensitized with 102.1F10 IgE (Fig. 3*C*). These data are consistent with loss of the nonclassical binding interaction, for which Arg7 is a key component, leaving only the classical site that alone is insufficient to induce cross-linking by monomeric *Phl p* 7.

Superantigen-Like Allergen Recognition. All the antibody contact residues for both sites are presented in Table 1 together with their genetic origin and whether they are germline encoded or derived through somatic hypermutation. The classical interaction site is dominated, as commonly observed, by residues generated by junctional diversity in CDR-H3, together with somatic mutations in CDR-H2 and CDR-L3. In contrast, the nonclassical site involves six residues from CDR-L2 and the adjacent framework FR-L3, with no involvement of the other CDRs; the similarity to autoantigen and superantigen binding is discussed below. Three asparagine residues in CDR-L2, Asn53, Asn54, and Asn55, contribute critical hydrogen bonds to main-chain atoms of the allergen, and a salt bridge and further hydrogen bonds are contributed by spatially adjacent framework residues Asp62, Lys68, and Thr78, as described above. Five of these six residues are germline encoded (Vλ1–40), but Asn54 is a somatic

mutation from serine. Intriguingly, this residue position, which is rarely involved in antigen binding, has been identified as a mutational hotspot from a comprehensive comparison of sequence data (22, 23). The S54N mutation thus contributes to the specificity for *Phl p* 7 recognition in the context of a region of germline-encoded residues that may predispose to *Phl p* 7 binding. Since the Vλ1-40 gene is one of the most frequently expressed genes of the Vλ1 family, and Asn54 is encoded in the germline sequence of other Vλ1 family members at this position, the motif responsible for the nonclassical interaction may be common in the antibody repertoire.

Discussion

The structure reported here demonstrates that an antibody can bind simultaneously to two identical protein antigens using both classical CDR-mediated binding and nonclassical FR-mediated binding. Furthermore, these two interactions engage epitopes on each of the *Phl p* 7 allergen molecules that are nonoverlapping, so that each *Phl p* 7 can be engaged simultaneously by two identical Fabs (Fig. 1 *A* and *B*). Both observations have implications for the triggering of cellular responses through cross-linking of antibodies, whether receptor bound or in membrane-bound form as part of the BCR.

Contrary to the current dogma that one antibody can recognize only a single epitope on an antigen (allergen), we have demonstrated here that a monomeric allergen *Phl p* 7 can indeed cross-link two identical FcεRI-bound anti-*Phl p* 7 IgE antibodies on a basophil and induce degranulation. We show by mutagenesis that this is the result of allergen recognition by the antibody using the nonclassical as well as the classical binding sites. This cross-linking mechanism is illustrated in Fig. 4. The antibody used in this work was originally expressed by the allergic patient as an IgG4, but we know that this patient also expressed *Phl p* 7-specific IgE (4) and that switching from IgG4 to IgE can occur as part of the response to allergen (24); however, we do not know whether this exact specificity was expressed naturally by the patient as IgE. Conversion of the IgG4 antibody to an IgE containing the identical matched VH and VL domains, reflecting the natural class-switching process that occurs in vivo, does not affect its affinity for *Phl p* 7, as shown previously (25) and in the present work.

An intriguing feature of the crystal structure is the presence of the second monomeric *Phl p* 7 molecule located between the two identical Fabs (Fig. 1*A*). There is no contact between the two monomers, but the way in which one monomer interacts with the two antibodies classically and nonclassically permits the other monomer to interact with the same two Fabs in a reciprocal manner, that is, each antibody simultaneously binds one *Phl p* 7 monomer classically and the other nonclassically. Thus, if one monomer first cross-links two IgE Fabs, a second would then readily bind, given that the two antibody binding sites are already disposed appropriately. The second monomer (but not behaving as a dimer) would thus strengthen the cross-linking in a manner akin to an avidity effect. This might be an essential feature of this alternative mode of cross-linking and involvement of the nonclassical site.

The dual specificity and FR-mediated binding also have implications for the BCR and potential B cell superantigen-like activity. A nonclassical mode of antibody recognition remarkably similar to that seen here for *Phl p* 7 has been reported previously in the structure of a rheumatoid factor (RF) IgM Fab fragment bound to the autoantigen IgG-Fc (26). The RF antibody contact residues included four that were germline encoded, one of which was in CDR-L2, and a single somatic mutation, also in CDR-L2, from serine to proline at position 56; this is the C-terminal residue of CDR-L2, immediately adjacent to the framework (FR-L3). This recognition site for the autoantigen in a location similar to that of the *Phl p* 7 interaction did not overlap with the classical

Fig. 3. Characterization of oligomeric state, affinity measurements, and basophil degranulation for *Phl p* 7 wild-type and R7T mutant. (*A*) Chromatograms of the RI signals for *Phl p* 7 wild-type (black trace) and mutant (green trace). The two proteins [in 25 mM Tris·HCl (pH 7.4) and 150 mM NaCl with 4 mM CaCl$_2$] were run over a Superdex 75 5/150 column (GE Healthcare) at a flow rate of 0.3 mL/min. The lines across the protein elution volume show the molecular masses of the *Phl p* 7 wild-type (black) and R7T mutant (green) proteins, indicating a monomeric state. The molecular masses as mean ± SD of three experiments for *Phl p* 7 wild-type and mutant are 12.4 ± 1.1 kDa and 10.8 ± 1.7 kDa (elution peaks 2.02 and 2.04 mL), respectively. (*B*) SPR sensorgrams showing the binding of *Phl p* 7 wild-type and mutant proteins to immobilized anti–lambda-biotin-102.1F10 IgE at concentrations of 5 nM (cyan), 10 nM (blue), 20 nM (green), 40 nM (red), and 80 nM (black). The affinities of *Phl p* 7 wild-type and mutant are 1.7×10^{-10} M and 6×10^{-10} M, respectively. (*C*) Basophil degranulation assay showing the percentage degranulation of RBL-SX38 basophils sensitized with 102.1F10 IgE and stimulated with 5,000 ng/mL of *Phl p* 7 wild-type, *Phl p* 7 mutant, or assay medium (background). Degranulation is expressed as a percentage of that induced by cell lysis. Bars represent the mean ± SEM of three independent experiments. Statistically significant difference to background was determined by one-way ANOVA with Tukey's posttest; ****$P < 0.0001$, nonsignificant (ns) $P > 0.05$.

antigen-binding site either. Although the primary specificity of the RF antibody was unknown, the structure suggested that simultaneous binding of the unknown antigen and the IgG-Fc autoantigen might be possible; this implied dual reactivity of the BCR was proposed as a contributing factor in the generation of the RF autoantibody (27). Furthermore, in a cryo-EM study of an anti-hepatitis B virus antibody Fab bound to the virus capsid, classical binding of the Fab to one antigen spike appeared to be enhanced

by simultaneous interaction through framework residues (including the same FR-L3 region as for *Phl p* 7) to an adjacent spike (28).

The dual reactivity that we see for our *Phl p* 7-specific antibody, in addition to the enhanced affinity for cross-linking described above, may also have functional implications for the original IgG4 antibody. IgG4 antibodies perform a protective role in allergy, blocking IgE binding to allergen epitopes (4): An antibody with dual reactivity for two different epitopes on the

Table 1. The genetic origin of the 102.1F10 Fab contact residues in the Fab/*Phl p* 7 complex

Segment	Contact residue	Antibody region	Genetic origin	Binding site
V$_H$ (V1–3)	S31	CDR H1	Germline	Classical
	Y32	CDR H1	Germline	Classical
	W47	CDR H2	Germline	Classical
	R50	CDR H2	Somatic mutation	Classical
	N52	CDR H2	Germline	Classical
D (D3–10)	F100	CDR H3	VDJ junction	Classical
	Y101	CDR H3	VDJ junction	Classical
	S103	CDR H3	VDJ junction	Classical
	S104	CDR H3	VDJ junction	Classical
	G105	CDR H3	VDJ junction	Classical
J$_H$ (J$_H$4)	—		—	—
V$_L$ (V$_\lambda$1–40)	Y33	CDR L1	Germline	Classical
	N53	CDR L2	Germline	Nonclassical
	N54	CDR L2	Somatic mutation	Nonclassical
	N55	CDR L2	Germline	Nonclassical
	D62	FR L3	Germline	Nonclassical
	K68	FR L3	Germline	Nonclassical
	T78	FR L3	Germline	Nonclassical
	F93	CDR L3	Somatic mutation	Classical
	W100	CDR L3	Germline	Classical
J$_L$ (J$_\lambda$4)	—		—	—

H, heavy chain; L, light chain; VDJ, variable diversity joining.

same allergen would, in principle, provide enhanced blocking activity for that allergen. IgG4 antibodies, uniquely, may also undergo Fab arm exchange (FAE) in which heavy chains of one antibody dissociate and reassociate with the heavy chains of another IgG4 antibody of a different specificity to generate a bispecific molecule (29–31). An IgG4 antibody with dual specificity in a single Fab arm could thus retain this property and even acquire an additional specificity following FAE. Such an antibody might have even greater blocking activity if the additional specificity is for allergen.

B cell superantigens that bind exclusively to FR residues and for which structural data are available include the VH-binding *Staphylococcus aureus* Protein A (1) and the VL-binding *Peptostreptococcus magnus* Protein L (2). These and other B cell superantigens such as protein Fv (32) contain multiple binding sites for V domains and therefore can cross-link either membrane-bound antibody in the BCR or FcεRI-bound IgE antibodies on mast cells and basophils. In this latter regard they have been described as superallergens (33); *S. aureus* enterotoxins have also been proposed to cross-link FcεRI-bound IgE molecules using both classical and FR-mediated binding (34, 35). The cross-linking of IgE antibodies reported here for *Phl p* 7 indicates that certain allergens, potentially including *Ole e* 3, which also induces degranulation as a monomer, may similarly act as superallergens by virtue of their ability to engage antibodies both classically and nonclassically. This may contribute to the potency of these allergens.

Although we were unable to measure the affinity of the FR-mediated binding of the antibody with *Phl p* 7 (*Materials and Methods*, *SPR*, and *SI Appendix*, Fig. S2) the relative interface areas suggest that this is much weaker than the subnanomolar affinity of the classical binding interaction. However, low-affinity antibody–epitope interactions can play a critical role in triggering mast cell or basophil activation (36); their synergy with high-affinity interactions has been studied with antibodies of known affinity to allergens [e.g., house dust mite *Der p* 2 (37)] as well as with model allergens displaying haptens and antihapten antibodies of known affinity (38). Weak interactions can contribute in this way to IgE cross-linking and cell activation because IgE, in contrast to IgG, with its uniquely high affinity for its Fc receptor

(FcεRI), is receptor bound at the cell surface with a locally high concentration before the appearance of the allergen. Similar considerations will apply to membrane-bound antibodies of all classes in their respective BCRs.

The structure reported here extends our understanding of how an antibody can recognize an antigen, and the dual reactivity also suggests possible mechanisms for antibody and/or BCR cross-linking relevant to disease. With respect to allergic disease and our understanding of allergenicity, it may also be important for informing the design of hypoallergenic molecules for allergen immunotherapy (39, 40) or antibodies for passive immunization (41).

Materials and Methods

Expression and Purification of Monoclonal IgEs and IgG1 Fab. *Phl p* 7-specific antibodies 102.1F10 and CS09G6K were generated by single B cell cloning and were converted from their original IgG4 and IgG2 subclasses, respectively, into IgE and, for 102.1F10, into IgG1, using polymerase incomplete primer extension (PIPE) cloning (42). Antibody 102.1F10 was isolated from the peripheral blood of a subject undergoing grass pollen immunotherapy (4). Antibody CS09G6K was derived from B cells isolated from a nasal biopsy sample from an allergic subject; nasal biopsy tissue was dissociated by enzymatic digestion for 1 h at 37 °C with 250 μg/mL Liberase (Roche), 50 μg/mL Hyaluronidase (Sigma), and 50 μg/mL DNase I (Roche). Single B cells were isolated by flow cytometry, and antibody variable regions were cloned and expressed as previously described (4). Samples were obtained following written informed consent of participants, and all experiments involving human subjects were approved by the East London and The City research ethics committee (approval 09/H0704/67). Matched VH and VL regions were amplified by RT-PCR from single B cell lysates. Sequences were obtained by capillary sequencing and were cloned into expression vectors containing corresponding human IgG1 or IgE constant regions for recombinant expression. For the expression of IgG1 Fab, FreeStyle MAX transfection reagent (Life Technologies) was used according to the manufacturer's instructions. Suspension- and serum-free–adapted FreeStyle 293-F cells (Life Technologies) were transfected. The Fab fragments were purified using a HisTrap HP column according to the manufacturer's instructions (GE Healthcare).

Allergen Protein Expression. The DNA for full-length *Phl p* 7, *Bet v* 4, and *Ole e* 3 was synthesized by MWG (Eurofins), codon optimized for expression in *Escherichia coli*. The DNA was cloned into a pET151 vector, which includes an N-terminal cleavable V5- and His-tag, according to the manufacturer's instructions (Life Technologies), and the sequence was verified. *Phl p* 7 DNA
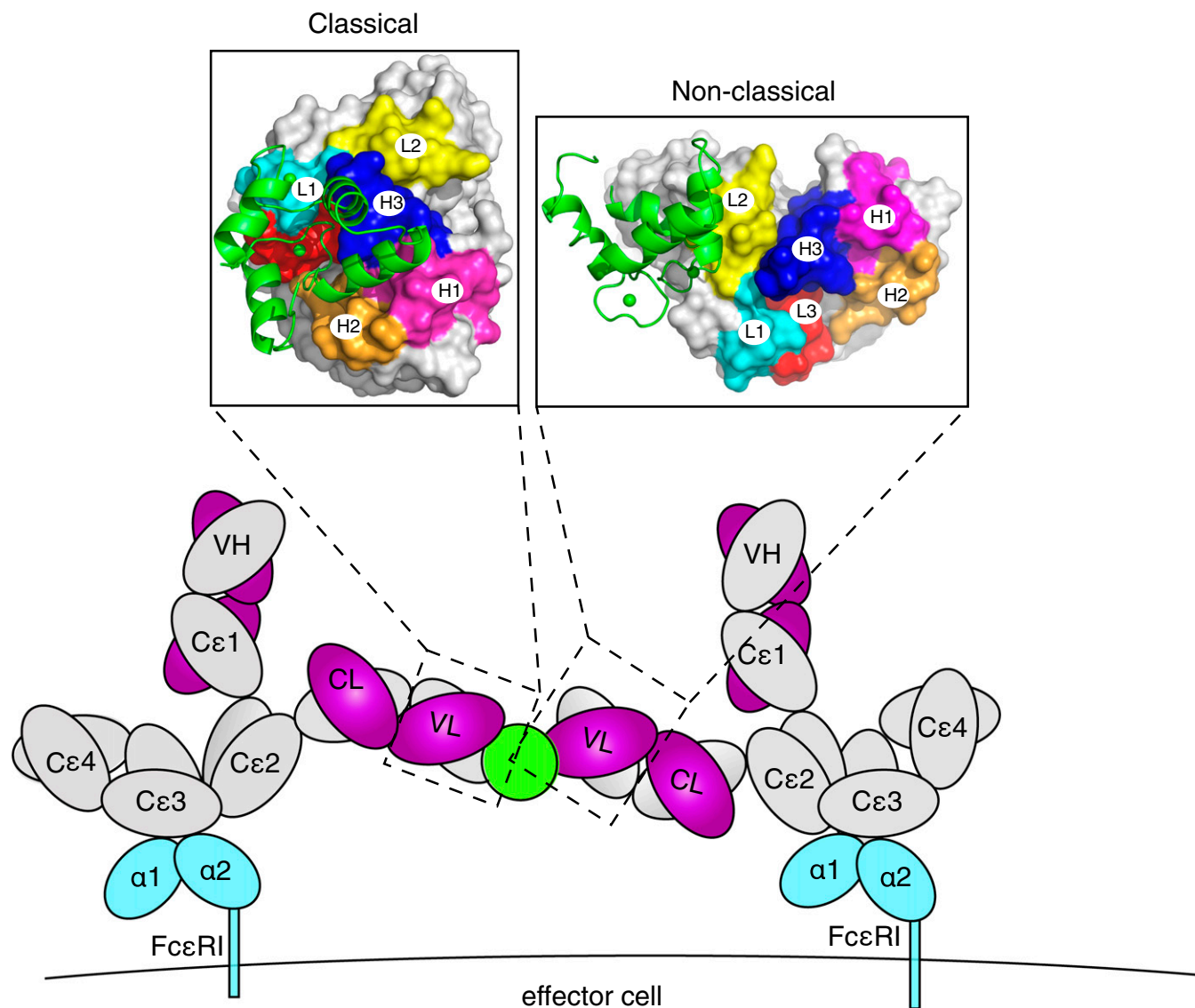
Fig. 4. Schematic mechanism of the cross-linking of two identical receptor-bound IgE antibodies by monomeric *Phl p* 7 on the cell surface. High-affinity receptor (cyan) and IgE (gray and magenta for heavy and light chain, respectively) complexes are cross-linked by allergen (green). The monomeric allergen binds to two distinct paratopes on IgE. (*Left*) The classical binding site involving all CDRs except CDR-L2 of the antibody. (*Right*) The other nonclassical, superantigen-like binding site involves only CDR-L2 and FR-L3 residues of the VL domain of the antibody. The *Insets* show the molecular details of the interaction between monomeric *Phl p* 7 (green cartoon) and the two identical *Phl p* 7-specific Fabs (white). CDRs of the heavy chain H1, H2, and H3 are labeled and colored magenta, orange, and blue, respectively; CDRs of the light chain L1, L2, and L3 are labeled and presented in cyan, yellow, and red, respectively.

was also cloned into a pET101 vector, which includes a C-terminal noncleavable V5- and His-tag. For expression, the plasmid was transformed into BL21 star DE3 (Life Technologies) and was plated on ampicillin overnight. The colonies were used to inoculate a 5-mL starter culture in Luria broth, with ampicillin; this culture was grown for 6 h and then was used to inoculate 250 mL ZYP-5052 autoinduction medium overnight (43). The bacteria were harvested by centrifugation at $4,000 \times g$ and then were lysed using BugBuster (Merck Millipore) according to the manufacturer's instructions. The soluble fraction had imidazole added to a final concentration of 10 mM and then was passed over a 1-mL HisTrap column (GE Healthcare) using an AKTA prime chromatography system (GE Healthcare Life Sciences) and was washed with Tris-buffered saline (TBS) buffer [25 mM Tris·HCl (pH 7.4), 300 mM NaCl, 4 mM CaCl$_2$] containing 10 mM imidazole. The protein was eluted using TBS (as above) containing 500 mM imidazole. A fraction of the His-V5-*Phl p* 7 protein was set for 8 h dialysis at 4 °C in a buffer containing 25 mM Tris·HCl (pH 7.4), 150 mM NaCl, 4 mM CaCl$_2$, 20 mM imidazole, 1 mM DTT, and tobacco etch virus (TEV) protease (0.2 mg) for the cleavage of the His-tag. The reaction mixture was then applied to a HisTrap column (GE Healthcare) to remove the cleaved tag. The concentrations of

His-V5-*Phl p* 7, His-V5-*Bet v* 4, and His-V5-*Ole e* 3 were determined with a DS-11 spectrophotometer (DeNovix). *Phl p* 7-V5-His and *Phl p* 7 (without the tag) contain no tyrosine or tryptophan residues and thus absorb poorly at 280 nm; therefore conventional spectroscopic detection was not useful. Fractions containing protein were identified by SDS gel electrophoresis, pooled, concentrated, and run over a Superdex 75 10/300 column (GE Healthcare) in TBS with 4 mM CaCl$_2$ and 0.1% sodium azide, monitoring the wavelength at 208 nm for the peptide backbone and at 257 nm for phenylalanine. Fractions from the peak corresponding to the allergen were pooled and concentrated for experimental use.

SPR. All experiments were carried out on a Biacore T200 instrument (GE Healthcare) at 25 °C. To measure the affinity of *Phl p* 7 and other cross-reactive allergens to 102.1F10 IgE, CaptureSelect biotinylated anti-lambda conjugate (Thermo Fisher Scientific) was immobilized onto a streptavidin chip (GE Healthcare). Then 2 nM 102.1F10 IgE was injected at 5 µL/min, and ~500 resonance units of the antibody were captured onto the anti-lambda surface. For CS09G6K IgE, CaptureSelect biotinylated anti-kappa conjugate (Thermo Fisher Scientific) was used under identical conditions. Different

concentrations of allergens were prepared by a twofold serial dilution in TBS buffer [25 mM Tris·HCl (pH 7.4), 150 mM NaCl, 4 mM CaCl$_2$, 0.005% surfactant P20]: *Phl p* 7 (twofold dilution series 0.35–500 nM), *Ole e* 3 (twofold dilution series 0.35–500 nM), *Bet v* 4 (twofold dilution series 4–1,600 nM). The samples were injected at 20 μL/min with an association phase of 180 s followed by a 10-min dissociation phase.

Purified 102.1F10 Fab was immobilized on a CM5 sensor chip by amine coupling. Allergens were injected over the surface for 240 s at a flow rate of 20 μL/min followed by a dissociation time of 900 s at a flow rate of 20 μL/min. Regeneration of the sensor surface was performed with a 60-s injection of 10 mM glycine-HCl (pH 2.5). These binding experiments were run in HBS buffer [10 mM Hepes (pH 7.4) 150 mM NaCl, 4 mM CaCl$_2$, and 0.005% surfactant P20]. Biacore T200 Evaluation software was used to analyze and present the data. Sensorgrams were all well fitted to a 1:1 stoichiometry model, including those for *Phl p* 7 binding to antibody 102.1F10 (*SI Appendix*, Fig. S4), which indicates that the affinity of the nonclassical interaction with this allergen is considerably weaker than that of the subnanomolar classical binding interaction and does not contribute to the sensorgram at the concentrations used here.

SEC-MALLS. Protein samples were first run over a Superdex 75 10/300 column (GE Healthcare), and the peak corresponding to the monomeric allergen was then used for SEC-MALLS analysis and the basophil degranulation assays. Before SEC-MALLS analysis the samples were dialyzed against 25 mM Tris·HCl and 150 mM NaCl TBS (pH 7.4) with 4 mM CaCl$_2$. For the SEC-MALLS analysis, protein samples were injected onto a Superdex 75 5/150 column (GE Healthcare) connected to an 1100 Series HPLC (Agilent Technologies). MALLS device detectors were normalized using TBS buffer (as above) supplemented with 4 mM CaCl$_2$ (pH 7.4) as the isotropic scattering agent; the flow rate was 0.3 mL/min. Each run was performed with 0.8 mg/mL of *Bet v* 4, 5 mg/mL of *Ole e* 3, 10 mg/mL of *Phl p* 7 wild-type, and 3 mg/mL of *Phl p* 7 mutant at 37 °C; the sample volume was 60 μL. Light-scattering and refractive index (RI) changes were monitored using a Viscotek SECMALS 20 (Malvern Instruments) multiangle light-scattering detector and a Viscotek VE3580 (Malvern Instruments) RI detector. Molecular weight and mass calculations were performed with the OMNISEC 5.02 software (Malvern Instruments). For the analysis of *Phl p* 7 complexes with 102.1F10 IgE (*SI Appendix*, Fig. S2), a Superdex 200 Increase 5/150 column (GE Healthcare) was used; buffer conditions were as described above. Light-scattering and RI changes were monitored using a miniDAWN (Wyatt Technology) multiangle light-scattering detector and an Optilab DSP (Wyatt Technology) RI detector. Molecular weight and mass calculations were performed with Astra 4.90 software (Wyatt Technology).

Basophil Degranulation Assay. RBL-SX38 cells, which express the human tetrameric form of FcεRI (44), were routinely cultured in RPMI medium supplemented with 10% FCS, 2 mM L-glutamine, 10 U penicillin/streptomycin, and 50 μg/mL Geneticin (all from Invitrogen) at 37 °C and 5% CO$_2$ in humidified air. RBL-SX38 cells were seeded at 1×10^4 cells per well in a 96-well plate in RPMI medium supplemented with 10% FCS, 2 mM L-glutamine, and 10 U penicillin/streptomycin and were incubated at 37 °C, 5% CO$_2$ in humidified air overnight. Following washing with HBSS (Invitrogen)/1% BSA (Sigma-Aldrich), cells were stimulated overnight by incubation with 200 ng/mL

IgE diluted in HBSS/1% BSA at 37 °C and 5% CO$_2$ in humidified air. Cross-linking of IgE-bound FcεRI was carried out by incubation with 50, 500, or 5,000 ng/mL allergen diluted in HBSS/1% BSA for 1 h at 37 °C and 5% CO$_2$ in humidified air. Supernatants were harvested for analysis. HBSS/1% BSA, polyclonal rabbit anti-human IgE (Dako), and HBSS/1% BSA/0.5% Triton X-100 (Sigma-Aldrich) were used as controls for background, crosslinking, and maximum degranulation, respectively. β-Hexosaminidase release was measured using 4-methylumbelliferyl *N*-acetyl-β-D-glucosaminide substrate (Sigma-Aldrich) as previously described (45), and degranulation was expressed as a percentage of the maximum degranulation induced by HBSS/1% BSA/0.5% Triton X-100.

Crystallization. Sitting-drop vapor diffusion crystallization screens were set up for the 102.1F10 Fab/*Phl p* 7 complex using a protein concentration of 3.7 mg/mL in a buffer comprising 25 mM Tris·HCl (pH 7.5), 20 mM NaCl, 4 mM CaCl$_2$, and 0.01% sodium azide. Crystals were grown at 18 °C using 100 μL reservoir solution comprising 0.1 M 2-(*N*-morpholino) ethanesulfonic acid (pH 6.5), 15% (wt/vol) PEG 6000, and 10% (vol/vol) 2-methyl-2,4-pentanediol. Crystals appeared after 5 d and were flash-cooled in liquid nitrogen using the reservoir supplemented with an additional 5% (vol/vol) 2-methyl-2,4-pentanediol as cryoprotectant.

Crystallographic Data Collection and Processing. Complete datasets were collected at beamline I02, Diamond Light Source (Harwell, United Kingdom). XDS (46) in Xia2 (47) and *aimless* (48) from the CCP4 Suite (49) were used to integrate and merge the data to a resolution of 2.35 Å. The crystal grew in space group P2$_1$, with unit cell dimensions a = 52.7 Å, b = 178.7 Å, c = 66.1 Å, and β = 94.8°. The structure was solved by molecular replacement with Phaser (50). To generate the 102.1F10 Fab search model, the BALBES database (51) was used to find the VL and Cλ domains from 3H42 and the CH1 and VH domains from 1RZF, from which the CDRs were removed manually. Iterative model building was performed in Coot (52) and refinement with PHENIX (53). Data processing and refinement statistics are summarized in *SI Appendix*, Table S1; the quality of the model was assessed with MolProbity (54). Structural figures were drawn using PyMOL (55). Coordinates and structure factors have been deposited in the Protein Data Bank under ID code 5OTJ.

1. Graille M, et al. (2000) Crystal structure of a Staphylococcus aureus protein A domain complexed with the Fab fragment of a human IgM antibody: Structural basis for recognition of B-cell receptors and superantigen activity. *Proc Natl Acad Sci USA* 97:5399–5404.
2. Graille M, et al. (2001) Complex between Peptostreptococcus magnus protein L and a human antibody reveals structural convergence in the interaction modes of Fab binding proteins. *Structure* 9:679–687.
3. Bueno C, Criado G, McCormick JK, Madrenas J (2007) T cell signalling induced by bacterial superantigens. *Chem Immunol Allergy* 93:161–180.
4. James LK, et al. (2012) Allergen specificity of IgG(4)-expressing B cells in patients with grass pollen allergy undergoing immunotherapy. *J Allergy Clin Immunol* 130:663–670.
5. Gould HJ, Sutton BJ (2008) IgE in allergy and asthma today. *Nat Rev Immunol* 8:205–217.
6. Hauser M, Roulias A, Ferreira F, Egger M (2010) Panallergens and their impact on the allergic patient. *Allergy Asthma Clin Immunol* 6:1–14.
7. Henzl MT, Sirianni AG, Wycoff WG, Tan A, Tanner JJ (2013) Solution structures of polcalcin Phl p 7 in three ligation states: Apo-, hemi-Mg^{2+}-bound, and fully Ca^{2+}-bound. *Proteins* 81:300–315.
8. Verdino P, Westritschnig K, Valenta R, Keller W (2002) The cross-reactive calcium-binding pollen allergen, Phl p 7, reveals a novel dimer assembly. *EMBO J* 21:5007–5016.
9. Niederberger V, et al. (1999) Calcium-dependent immunoglobulin E recognition of the apo- and calcium-bound form of a cross-reactive two EF-hand timothy grass pollen allergen, Phl p 7. *FASEB J* 13:843–856.
10. Rouvinen J, et al. (2010) Transient dimers of allergens. *PLoS One* 5:e9037.
11. Niemi MH, et al. (2015) Dimerization of lipocalin allergens. *Sci Rep* 5:13841.
12. Kofler S, et al. (2014) Stabilization of the dimeric birch pollen allergen Bet v 1 impacts its immunological properties. *J Biol Chem* 289:540–551.
13. Niemi M, et al. (2007) Molecular interactions between a recombinant IgE antibody and the beta-lactoglobulin allergen. *Structure* 15:1413–1421.
14. Li M, et al. (2008) Crystal structure of a dimerized cockroach allergen Bla g 2 complexed with a monoclonal antibody. *J Biol Chem* 283:22806–22814.
15. Gieras A, et al. (2016) IgE epitope proximity determines immune complex shape and effector cell activation capacity. *J Allergy Clin Immunol* 137:1557–1565.
16. Gadermaier E, et al. (2016) Epitope specificity determines cross-protection of a SIT-induced IgG4 antibody. *Allergy* 71:36–46.
17. Krissinel E, Henrick K (2007) Inference of macromolecular assemblies from crystalline state. *J Mol Biol* 372:774–797.
18. Henzl MT, Davis ME, Tan A (2010) Polcalcin divalent ion-binding behavior and thermal stability: Comparison of Bet v 4, Bra n 1, and Bra n 2 to Phl p 7. *Biochemistry* 49:2256–2268.
19. Neudecker P, et al. (2004) Solution structure, dynamics, and hydrodynamics of the calcium-bound cross-reactive birch pollen allergen Bet v 4 reveal a canonical monomeric two EF-hand assembly with a regulatory function. *J Mol Biol* 336:1141–1157.
20. Verdino P, et al. (2008) Three-dimensional structure of the cross-reactive pollen allergen Che a 3: Visualizing cross-reactivity on the molecular surfaces of weed, grass, and tree pollen allergens. *J Immunol* 180:2313–2321.

IMMUNOLOGY AND INFLAMMATION

21. Magler I, Nüss D, Hauser M, Ferreira F, Brandstetter H (2010) Molecular metamorphosis in polcalcin allergens by EF-hand rearrangements and domain swapping. *FEBS J* 277:2598–2610.

22. Lefranc MP, et al. (2015) IMGT®, the international ImMunoGeneTics information system® 25 years on. *Nucleic Acids Res* 43:D413–D422.

23. Sela-Culang I, Kunik V, Ofran Y (2013) The structural basis of antibody-antigen recognition. *Front Immunol* 4:302.

24. Cameron L, et al. (2003) S ε S μ and S ε S γ switch circles in human nasal mucosa following ex vivo allergen challenge: Evidence for direct as well as sequential class switch recombination. *J Immunol* 171:3816–3822.

25. Dodev TS, et al. (2015) Inhibition of allergen-dependent IgE activity by antibodies of the same specificity but different class. *Allergy* 70:720–724.

26. Corper AL, et al. (1997) Structure of human IgM rheumatoid factor Fab bound to its autoantigen IgG Fc reveals a novel topology of antibody-antigen interaction. *Nat Struct Biol* 4:374–381.

27. Sutton B, Corper A, Bonagura V, Taussig M (2000) The structure and origin of rheumatoid factors. *Immunol Today* 21:177–183.

28. Watts NR, et al. (2008) Non-canonical binding of an antibody resembling a naïve B cell receptor immunoglobulin to hepatitis B virus capsids. *J Mol Biol* 379:1119–1129.

29. Aalberse RC, Schuurman J (2002) IgG4 breaking the rules. *Immunology* 105:9–19.

30. van der Neut Kolfschoten M, et al. (2007) Anti-inflammatory activity of human IgG4 antibodies by dynamic Fab arm exchange. *Science* 317:1554–1557.

31. Davies AM, Sutton BJ (2015) Human IgG4: A structural perspective. *Immunol Rev* 268:139–159.

32. Bouvet JP, Marone G (2007) Protein Fv: An endogenous immunoglobulin superantigen and superallergen. *Chem Immunol Allergy* 93:58–76.

33. Marone G, et al. (2007) Role of superallergens in allergic disorders. *Chem Immunol Allergy* 93:195–213.

34. Gould HJ, Takhar P, Harries HE, Chevretton E, Sutton BJ (2007) The allergic march from Staphylococcus aureus superantigens to immunoglobulin E. *Chem Immunol Allergy* 93:106–136.

35. Chen JB, et al. (2017) Antibodies and superantibodies in patients with chronic rhinosinusitis with nasal polyps. *J Allergy Clin Immunol* 139:1195–1204.

36. Sutton BJ (2013) Immunology: Allergy's Achilles' heel? *Nat Chem Biol* 9:757–759.

37. Christensen LH, Holm J, Lund G, Riise E, Lund K (2008) Several distinct properties of the IgE repertoire determine effector cell degranulation in response to allergen challenge. *J Allergy Clin Immunol* 122:298–304.

38. Handlogten MW, Kiziltepe T, Serezani AP, Kaplan MH, Bilgicer B (2013) Inhibition of weak-affinity epitope-IgE interactions prevents mast cell degranulation. *Nat Chem Biol* 9:789–795.

39. Linhart B, et al. (2015) Molecular evolution of hypoallergenic hybrid proteins for vaccination against grass pollen allergy. *J Immunol* 194:4008–4018.

40. Focke-Tejkl M, et al. (2015) Development and characterization of a recombinant, hypoallergenic, peptide-based vaccine for grass pollen allergy. *J Allergy Clin Immunol* 135:1207–1217.

41. Flicker S, Linhart B, Wild C, Wiedermann U, Valenta R (2013) Passive immunization with allergen-specific IgG antibodies for treatment and prevention of allergy. *Immunobiology* 218:884–891.

42. Dodev TS, et al. (2014) A tool kit for rapid cloning and expression of recombinant antibodies. *Sci Rep* 4:5885.

43. Studier FW (2005) Protein production by auto-induction in high density shaking cultures. *Protein Expr Purif* 41:207–234.

44. Wiegand TW, et al. (1996) High-affinity oligonucleotide ligands to human IgE inhibit binding to Fc epsilon receptor I. *J Immunol* 157:221–230.

45. Bax HJ, Bowen H, Dodev TS, Sutton BJ, Gould HJ (2015) Mechanism of the antigen-independent cytokinergic SPE-7 IgE activation of human mast cells in vitro. *Sci Rep* 5:9538.

46. Kabsch W (2010) XDS. *Acta Crystallogr D Biol Crystallogr* 66:125–132.

47. Winter G, Lobley CM, Prince SM (2013) Decision making in xia2. *Acta Crystallogr D Biol Crystallogr* 69:1260–1273.

48. Evans PR, Murshudov GN (2013) How good are my data and what is the resolution? *Acta Crystallogr D Biol Crystallogr* 69:1204–1214.

49. Winn MD, et al. (2011) Overview of the CCP4 suite and current developments. *Acta Crystallogr D Biol Crystallogr* 67:235–242.

50. McCoy AJ, et al. (2007) Phaser crystallographic software. *J Appl Cryst* 40:658–674.

51. Long F, Vagin AA, Young P, Murshudov GN (2008) BALBES: A molecular-replacement pipeline. *Acta Crystallogr D Biol Crystallogr* 64:125–132.

52. Emsley P, Lohkamp B, Scott WG, Cowtan K (2010) Features and development of Coot. *Acta Crystallogr D Biol Crystallogr* 66:486–501.

53. Zwart PH, et al. (2008) Automated structure solution with the PHENIX suite. *Methods Mol Biol* 426:419–435.

54. Chen VB, et al. (2010) MolProbity: All-atom structure validation for macromolecular crystallography. *Acta Crystallogr D Biol Crystallogr* 66:12–21.

55. DeLano WL (2002) The PyMOL Molecular Graphics System (DeLano Scientific, Palo Alto, CA), Version 2.0.